Computer and Decision Making
An International Journal

Journal homepage: www.comdem.org
eISSN: 3008-1416

Study on offshore wind profile based on neutral equivalent wind speed

Xiaomei Ma, Yuting Dong, Jiaoli Jiao*

School of Physical and Electronic Information Engineering, Qinghai Normal University, Xining, Qinghai, 810016, China

ARTICLE INFO

Article history:
Received 17 April 2025
Received in revised form 19 May 2025
Accepted 22 May 2025
Available online 23 May 2025

ABSTRACT

To address the issue of extrapolation inaccuracy when the hub height of offshore wind turbines exceeds the measurement height of meteorological masts, this study proposes an offshore wind profile model based on neutral equivalent wind speed by comprehensively considering the Monin-Obukhov similarity theory and sea surface dynamic roughness. First, the effects of wind shear exponent, atmospheric stability, and turbulence intensity on offshore wind resources were investigated. Then, the proposed model was validated using measurement data from an offshore meteorological mast in Dalian. Compared with traditional extrapolation methods, the model yields annual average wind speed and wind power density at hub height that are closer to measured values, with root mean square error and mean absolute error of wind speed being 0.43 m/s and 0.28 m/s respectively. Moreover, the model effectively reflects the influence of sea surface dynamic roughness and atmospheric stability variations on vertical wind speed distribution, overcoming the limitations of conventional wind shear power law. This provides a scientific basis for offshore wind resource assessment and preliminary planning of wind farms.

Keywords:
atmospheric stability; wind speed of hub height; extrapolation; wind resource assessment

1. Introduction

China possesses abundant and stable offshore wind resources, with the added advantage of proximity to major load centers and minimal land occupation requirements[4]. These favorable conditions have positioned offshore wind power as a key focus area in China's renewable energy development in recent years. However, the feasibility assessment of such projects remains challenging due to two primary factors: the complex meteorological characteristics of offshore wind patterns and the current developmental stage of evaluation technologies[10]. Consequently, enhancing the accuracy of offshore wind resource assessment has become crucial for mitigating investment risks in offshore wind projects while strengthening their core competitiveness.

The underlying surface of the marine atmospheric boundary layer is the complex sea surface, and the study of parameterized models of ocean surface conditions is helpful to understand the physical processes of the offshore atmospheric boundary layer in depth, so as to improve the accuracy of off-

*email: jjl187973@163.com
Doi: https://www.doi.org/10.59543/comdem.v2i.14245

shore wind resource assessment. Charnock[2] and Smith[13] first proposed a parameterized model of ocean surface roughness, and established a linear model between friction velocity and roughness. Literature[1] studied the influence of different sea surface dynamic roughness parameterized models on the numerical simulation of vertical profiles of meteorological elements such as wind and temperature. Atmospheric stability is an important factor affecting the distribution of offshore wind resources. Literature[12] studied the influence of atmospheric stability on the spatial and temporal distribution of wind resources. Literature[17] analyzed and compared the applicability of different classification standards of atmospheric stability to the calculation of wind shear index in coastal areas, and reached the conclusion that there is a high correlation between wind shear index and atmospheric stability. Literature[6] found that atmospheric stability has a great influence on wind farm power output according to modeling of wind farms. In Literature[18], the characteristics of turbulence intensity in the north coast of Bohai Bay were analyzed based on the observation data of wind tower, and suggestions for adjusting anti-turbulence parameters of wind turbines were put forward. However, when studying the characteristics of offshore wind resources in the above literatures, a single parameter is used to describe them, and some studies directly use the parameterized model of sea surface dynamic roughness to fit the offshore wind profile, ignoring the assumption that the atmosphere in the model is always in neutral stratification. In fact, the state of the ocean surface changes all the time, and the period of atmospheric neutral stratification rarely occurs. This approximation method will bring errors in wind resource assessment, resulting in the deviation between the design value of the whole field power generation and the actual operating value[9]. This paper introduces the concept of neutral equivalent wind speed, which converts the instantaneous wind speeds under both stable and unstable atmospheric conditions into equivalent wind speeds under neutral conditions, combining M-O similarity theory and kinetics of ocean surface roughness parametric model to describe the vertical distribution of the offshore wind resources, to enhance offshore wind resource assessment accuracy, reduction of offshore wind power project investment risk.

2. Research on offshore wind resource assessment parameters and models

2.1 Atmospheric stability parameter model

Both Monin-Obukhov length L and Gradient Richardson number R_i are parameters of atmospheric stability. The gradient Richardson number is calculated with the discrete data obtained from actual observations as follows [5]:

$$R_i = \frac{g}{\bar{T}}\left(\Delta T/\sqrt{z_1 z_2 \ln\frac{z_2}{z_1}} + \Gamma_d\right)\left(\sqrt{z_1 z_2}\ln\frac{z_2}{z_1}/\Delta\bar{u}\right)^2 \tag{1}$$

Where, $z_1 z_2$ is different heights, ΔT is the absolute temperature difference between two heights, Γ_d is the dry adiabatic temperature reduction rate, $\Delta\bar{u}$ is the wind speed difference between two heights, and $\bar{T}$ is the average absolute temperature of two heights.

$$L = \begin{cases} \frac{z}{R_i} & \text{stable} \\ \frac{z(1-5R_i}{R_i} & \text{unstable} \end{cases} \tag{2}$$

2.2 Parametric model of friction velocity

Friction velocity is an important factor when studying the interaction between ocean and atmosphere, and , it can be obtained based on the Reynolds stress relationship by using the average wind

speed at the height of 10 m and drag coefficient[15, 16, 19]:

$$u_*^2 = C_d U_{10}^2 \tag{3}$$

The drag coefficient determines the momentum transfer rate between the atmosphere and ocean, which varies with the wind speed, and is related to the surface roughness and atmospheric stability [3]. The parameterized model of drag coefficient considered in this paper is Largeand Pond model[8]:

$$C_d = \begin{cases} 1.2 \times 10^{-3}, & 0 < U_{10} \leq 11 \text{ m/s} \\ (0.49 + 0.065U_{10}) \times 10^{-3}, & 11 < U_{10} < 25 \text{ m/s} \\ 2.1 \times 10^{-3}, & U_{10} \geq 25 \text{ m/s} \end{cases} \tag{4}$$

2.3 *Parametric model of ocean surface dynamic roughness*

Charnock[2] first proposed the relationship between sea surface roughness and friction velocity:

$$z_0 = \alpha \frac{u_*^2}{g} \tag{5}$$

Where, $\alpha = 0.0185$. Charnock model has been widely used, and subsequent studies on parameterization schemes are basically carried out on this basis. Smith[13] adds the influence of smooth sea surface current to the Charnock model:

$$z_0 = \alpha \frac{u_*^2}{g} + 0.1 \frac{v}{u_*} \tag{6}$$

Charnock model is adopted in this paper for it can simulate the physical process of the maritime boundary layer well.

2.4 *Wind profile model at different levels of stability*

The integral form of flux-profile relationship of wind speed near the surface layer obtained by the Monin-Obukhov similarity theory is as follows:

$$u(z) = \frac{u_*}{k} \left(\ln \frac{z}{z_0} - \psi_m \right) \tag{7}$$

Where, ψ_m is the correction function of wind profile stability, z_0 is the ocean surface dynamic roughness, u_* is the friction velocity, k is the von Karman coefficient, 0.4.

$$\psi_m = \begin{cases} -\frac{5z}{L} & \text{stable} \\ 0 & \\ 2\ln\left(\frac{1+x}{2}\right) + \ln\left(\frac{1+x^2}{2}\right) - 2\arctan\left(x + \frac{\pi}{2}\right) & \text{unstable} \end{cases} \tag{8}$$

Among, $x = \left(1 - \frac{16z}{L}\right)^{1/4}$.

3. Offshore wind profile model based on neutral equivalent wind speed

Both the existing parameterized model of sea surface dynamic roughness and wind resource assessment software assume that the atmosphere always keep neutral state due to the limitation of

modeling difficulty and calculation speed, which limits the further improvement of assessment accuracy to some extent[7]. At present, the hub height of onshore wind turbines even has exceeded 160 meters, which is higher than the wind mast height, and the consequence is that hub height wind speed has to be extrapolated from measurement height at the wind resource assessment stage. For the above reasons, in order to satisfy the assumptions of some models and evaluation software on the atmospheric state, an offshore wind profile model based on neutral equivalent wind speed is proposed in this paper.

3.1 Offshore wind profile model based on neutral equivalent wind speed

Assume u_{zn} is the wind speed at wind measurement height z under neutral condition, then:

$$u_{zn} = \frac{u_*}{k} \ln \frac{z}{z_0} \tag{9}$$

Joint Equation (7) and (9),

$$u_{zn} = u(z) + \frac{u_*}{k} \psi_m \tag{10}$$

Where, $u(z)$ is the measured wind speed at the wind measurement height z, and ψ_m is the stability function.

Considering the convenience of calculation and data availability, this paper with two layers by the wind speed, temperature data calculation gradient Richardson number and mo the length, judge the atmospheric stability classification and time by time ψ_m into Equation (10), the time into the neutral equivalent wind speed, the equivalent wind speed of the neutral equivalent transformation by time, can satisfy some model and the evaluation software assumption of the atmospheric state.

It is assumed that u_{1n} is the equivalent wind speed under neutral state corresponding to height z_1, and z_2, u_2 are respectively the hub height and corresponding wind speed which need to be extrapolated. Since the equivalent transformation of wind speed at lower height layer has been done, logarithmic rate under neutral state is used for extrapolation in this paper, namely:

$$u_2 = \frac{u_{1n} (\ln z_2 - \ln z_0)}{\ln z_1 - \ln z_0} \tag{11}$$

Joint Equation (10),

$$u_2 = \frac{\left(u_1 + \frac{u_*}{k}\psi_m\right) (\ln z_2 - \ln z_0)}{\ln z_1 - \ln z_0} \tag{12}$$

In the above formula, z_0 adopts Charnock model, that is:

$$u_2 = \frac{\left(u_1 + \frac{u_*}{k}\psi_m\right) \left(\ln z_2 - \ln \alpha \frac{u_*^2}{g}\right)}{\ln z_1 - \ln \alpha \frac{u_*^2}{g}} \tag{13}$$

Equation (13) is the offshore wind profile model based on neutral equivalent wind speed. As the wind speed at the height z_1 adopts the neutral equivalent wind speed, the atmospheric state and the dynamic roughness of the sea surface have been considered as the factors at the lower height layer, so the extrapolated wind speed at the height is close to the actual state. Compared with the method of extrapolating hub height wind speed directly using the lower height wind speed, the model comprehensively considers the influence of atmospheric stability and sea surface dynamic roughness on the offshore wind profile, and the result is more close to the actual situation, which reduces the calculation error caused by extrapolation. Fig. 1 is the flow chart of the offshore wind profile model based on neutral equivalent wind speed.

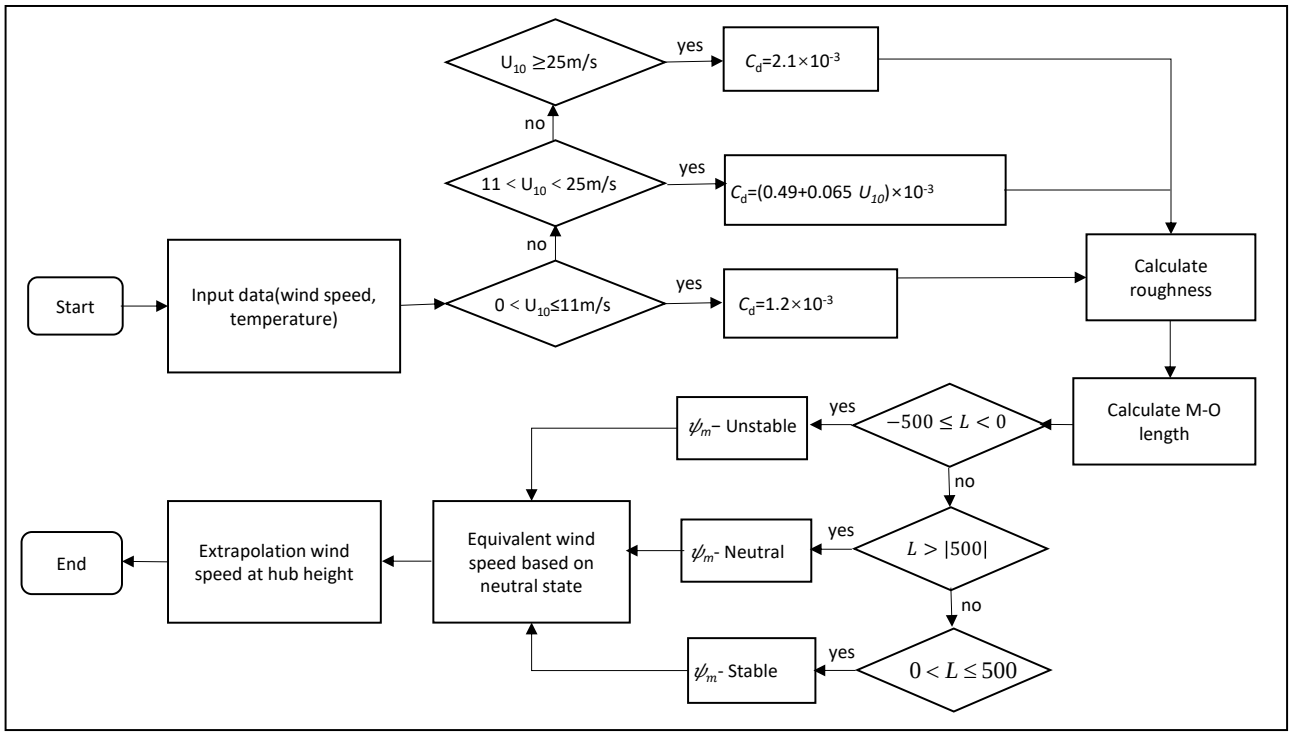

Fig. 1. Flow chart of proposed model

3.2 Model evaluation index

In practical application, root mean square error($RMSE$) and mean absolute error(MAE) can be used to measure the deviation between the predicted value and the true value. Therefore, these two indexes are used in this example to evaluate the accuracy of the model. The calculation formula is as follows:

$$RMSE = \sqrt{\frac{\sum_{i=1}^{n} \left(v_{real,i} - v_{ettrapolation,i}\right)^2}{n}} \tag{14}$$

$$MAE = \frac{1}{n} \sum_{i=1}^{n} \left| v_{real,i} - v_{extrapolation,i} \right| \tag{15}$$

Where, $v_{real,i}$ is the measured wind speed value for the first time, $v_{extrapolation,i}$ is the extrapolated wind speed value for the second time, and n is the total number of measurements.

4. Case analysis

4.1 Offshore mast information

The wind mast data of an offshore wind farm in China is taken as an example to verify the offshore wind profile model based on neutral equivalent wind speed proposed in this paper. The wind tower is located near Da Nan Island in the north of the Yellow Sea. The data collection time series is from January 1th, 2016 to December 31th, 2016, and the sampling period is 10min. The data includes the mean, maximum, minimum, and variance within each channel. The integrity rate of the original data is reaching more than 95%. According to the national standard GB/T18710-2002 and the industry

standard NB/T 31147-2018, the integrity rate reaches 100% after data interpolation. Tab.1 shows the basic information of the wind tower.

Table 1
Information of wind mast

Variable	Value
Latitude	$39°35'\mathrm{N}$
Longitude	$123°19'\mathrm{E}$
Start date	$2016/1/1\ 00:00$
End date	$2016/12/31\ 23:50$
Length of time step	10 minutes
Mean temperature	$10.2°\mathrm{C}$
Mean air density	$1.232\ \mathrm{kg/m^3}$
Power law exponent	0.0532

4.2 Distribution of offshore wind resources

4.2.1 Atmospheric stability parameters and classification

Atmospheric stability is the main thermal factor that causes the vertical variation of wind speed. According to Equation (1) and (2), the hourly gradient Richardson number and Monin-Obkhov length are calculated, and the atmospheric state is classified by using the classification standard in Tab.2.

Table 2
Standard of atmospheric stability classification

Stability	L
Unstable	$-500 \leq L < 0$
Neutral	$L > \lvert 500 \rvert$
Stable	$0 < L \leq 500$

The classification of atmospheric state is counted in order to verify the accuracy of the classification of atmospheric stability and ensure the accuracy of extrapolation. Fig. 2 shows the hourly classification of atmospheric stability, and Fig. 3 shows the classification of atmospheric stability in different seasons. It can be seen that the proportion of neutral state is not high at any time scale. In Fig.1, the proportion of unstable condition at noon and stable condition at night are higher than that at other times. Generally speaking, the proportion of unstable state in the atmosphere is larger throughout the year.

In general, the temperature in the surface layer decreases with the increase of height, and the phenomenon that the temperature increases with the increase of height is called temperature inversion. An inversion layer can form over the sea when warmer air from land flows in advection over the cooler sea. The existence of inversion layer prevents the vertical movement of airflow and keeps the atmosphere in a stable state, and the thicker the inversion layer, the greater the influence. The stable state proportion is significantly higher than other seasons in Fig.3. The moment of temperature inversion phenomenon occurring in the distribution of each season has been counted up in Tab.3 to analysis the reason for the above phenomenon. The result show that the temperature inversion phenomenon in spring is significantly higher than other seasons, which indicates that higher percentage

of stable condition in spring may be caused by the temperature inversion phenomenon, and shows that the atmospheric stability classification is accurate.

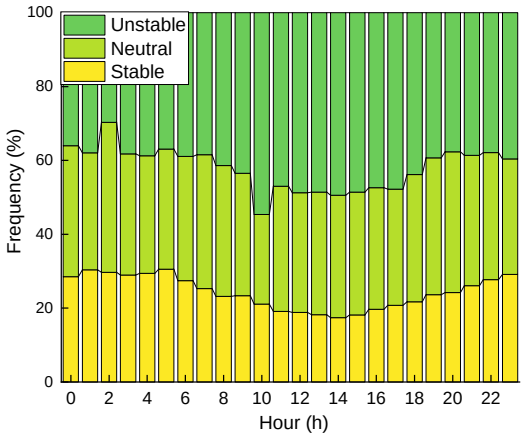

Fig. 2. Classification of atmospheric stability by hour

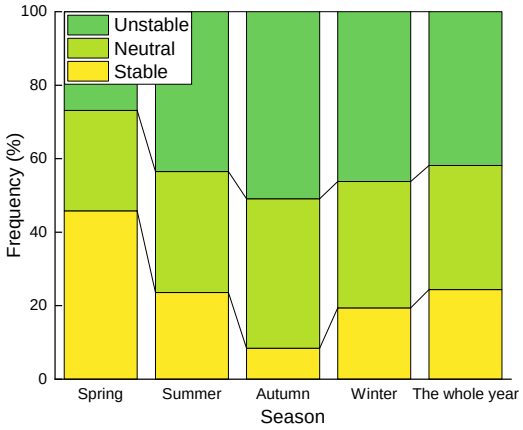

Fig. 3. Classification of atmospheric stability by season

Table 3
Proportion of temperature inversion

Season	Spring	Summer	Autumn	Winter	The whole year
Proportion	7.85%	3.08%	1.20%	3.22%	15.35%

Fig. 4 and Fig. 5 show measured wind speed at different heights and wind speed correlation analysis at 70 m and 90 m respectively. As can be seen from Fig. 4, the wind speed at 10 meters is significantly different from that at other heights, and the wind speed difference at other heights, especially above 60 meters, is small. It can be seen that the change of offshore wind energy resources with height is small. This law also indicates that when extrapolating the wind speed, the wind speed of the near altitude layer should be taken as the reference wind speed as far as possible. Fig.5 is the correlation of wind speed between the reference height of 70 meters and the extrapolation height of 90 meters to be adopted in this paper.

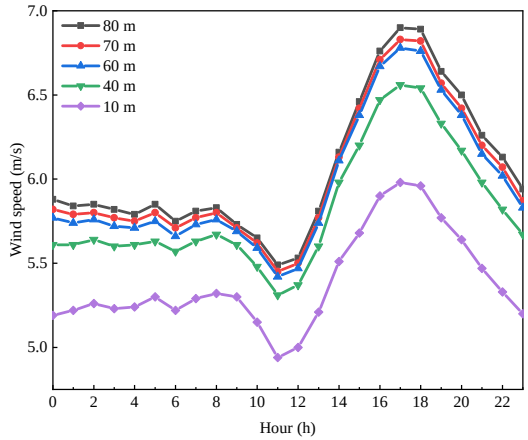

Fig. 4. Wind speed of different heights

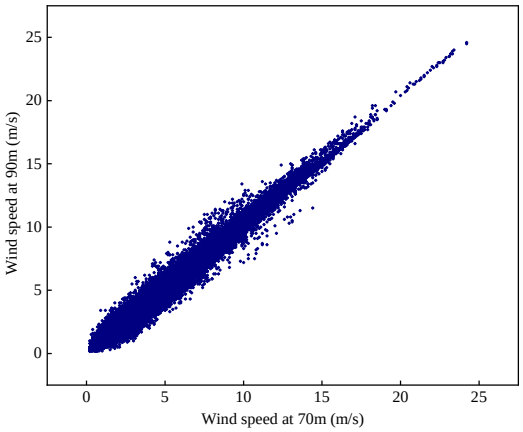

Fig. 5. The relevance of wind speed 70m and 90m

4.2.2 *Wind shear exponent*

Wind shear exponent reflects the variation of wind speed with the increase of height, which caused by turbulence viscosity and underlying surface friction. It is an important basis for determining the type selection and hub height of wind turbines in wind farms.

The wind shear exponent of different height intervals has been calculated and shown in Fig. 6. The average wind shear exponent of the whole wind farm is 0.0532, which is significantly lower than most values of onshore wind farms. The vertical wind shear exponent variation trends remained consistent across different height layers, though negative shear occurred at certain altitudes during December and January. Due to stable atmospheric conditions, significant discrepancies in wind shear exponents were observed between altitude levels.

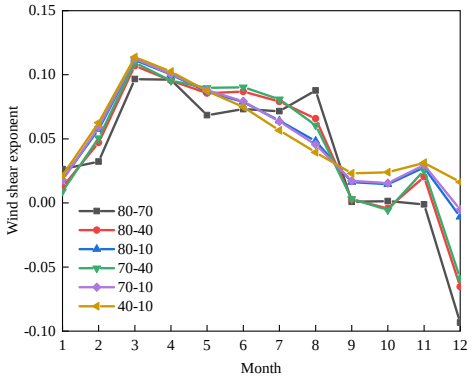

Fig. 6. Wind shear exponent at different height interval

4.2.3 *Turbulence intensity*

Turbulence intensity is the magnitude of random variation of wind speed within 10min, reflecting the fluctuation of wind speed[14]. There are two main reasons for turbulence. One is the friction or retardation of sea surface roughness during airflow, and the other is the vertical movement of airflow caused by the difference between air density and atmospheric temperature[11]. These two reasons exactly correspond to the influence of sea surface dynamic roughness and atmospheric stability. Fig. 7 shows the wind profiles under different atmospheric stability and Fig. 8 shows the turbulence intensity under different atmospheric stability.

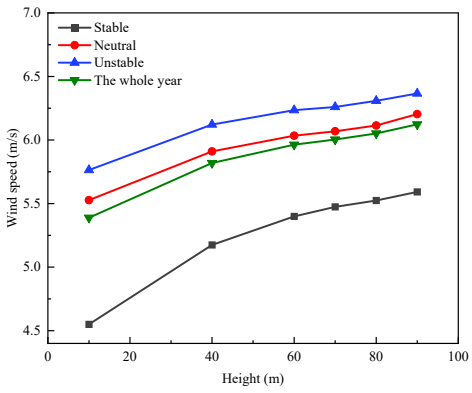

Fig. 7. Wind profile of different atmospheric stability

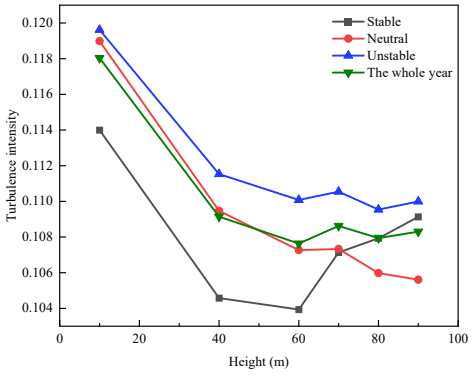

Fig. 8. Turbulence intensity of different atmospheric stability

The annual average wind speed and annual average turbulence intensity of the wind farm of 90m are 6.122m/s and 0.108, respectively. It can be seen from Fig. 7 and Fig. 8 that atmospheric stability affects the vertical distribution of wind speed and turbulence intensity. In summary, the variation of wind speed and turbulence intensity with height is opposite, and both are affected by atmospheric stability. Under the stable condition, the change of turbulence intensity is not completely consistent with the change rule that the higher the height is, the smaller the turbulence intensity is because of the less vertical exchange between the layers. The vertical distribution of wind speed and turbulence intensity under neutral condition is closest to the annual average level, which is the basis for traditional wind resource assessment to assume that atmospheric state is neutral. However, in order to further improve the economy and stability of wind power project landing, the influence of atmospheric stability on various parameters of wind resource assessment should be fully considered.

4.3 Model calculation results

In order to verify the practical application effect of the offshore wind profile model based on the neutral equivalent wind speed proposed in this paper, two methods were used to extrapolate the wind speed at the hub height respectively, and compared with the actual wind speed at the hub height. The accuracy of the different methods was evaluated by the selected evaluation indexes, and the hub height was set as 90m and the wind speed was extrapolated from 70m.

Method 1: The conventional extrapolation approach in wind resource assessment, that applies the site-wide average wind shear exponent to extrapolate hub-height wind speed.

Method 2: The offshore wind profile model based on neutral equivalent wind speed (as proposed in this study) is employed for hub-height wind speed extrapolation.

Tab.4 shows the average wind speed obtained by the two methods respectively and the Weibull distribution parameters of wind speed fitted by the least square method. Fig.9 show the root mean square error and mean absolute error of wind speed and wind power density.

Table 4
Offshore wind resource parameters by different extrapolations

	Mean wind speed (m/s)	Wind power density (w/m^2)	Shape parameter k	Scale parameter
Method 1	6.085	282.0	2.013	6.812
Method 2	6.092	287.0	1.998	6.815
Measured	6.123	287.8	1.984	6.856

As can be seen from the data in Tab.4, the annual average wind speed extrapolated from Method 1 and Method 2 is close to the measured value, while that from Method 2 is closer, but the difference is small. Method 2 advantage is mainly manifested in the wind power density and the calculation of the wind speed distribution parameters, compared with the annual average wind speed, method 2 average wind power density is calculated and measured values fitting degree is higher, and in the offshore wind farm capacity calculation, the wind power density is the more important factor, so the method 2 can be well simulated sea wind vertical distribution of resources. The main reason for the unsatisfactory result of method 1 is that the effect of atmospheric stability and sea surface dynamic roughness is ignored by the whole-field mean wind shear exponent.

As evidenced in Fig.9, the proposed neutral equivalent wind speed-based offshore wind profile model demonstrates superior accuracy in hub-height wind speed extrapolation compared to conventional methods. Both the time-series RMSE and MAE metrics for wind speed and wind power density are consistently lower than those of Method 1. Specifically, the annual average RMSE and MAE for

wind speed reach 0.43 m/s and 0.28 m/s respectively, indicating closer alignment with measured values than traditional approaches.

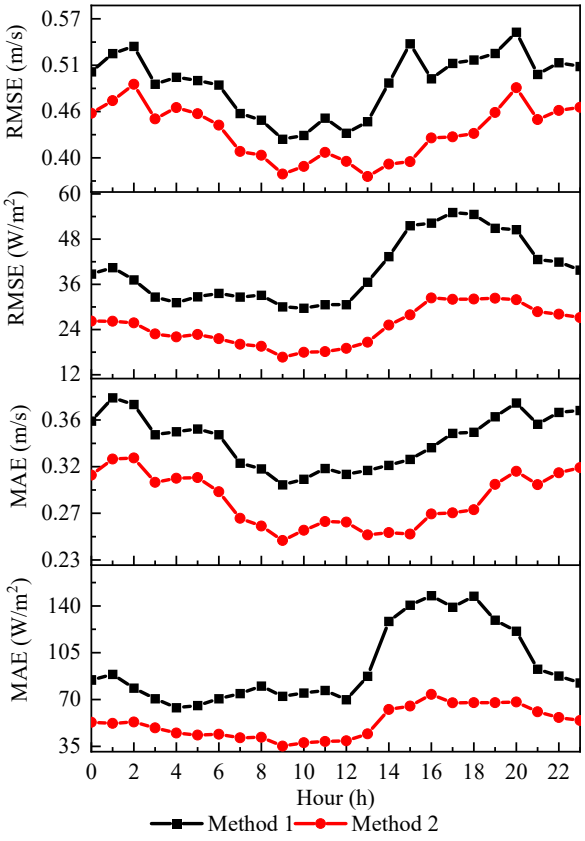

Fig. 9. RMSE and MAE of wind speed and wind power density

These results confirm that the neutral equivalent wind speed model achieves optimal computational performance in practical extrapolation scenarios, establishing a reliable reference framework for enhanced precision in offshore wind resource assessment.

5. Conclusions

Aiming at the problem that the hub height of offshore wind turbine is higher than the height of wind tower and the extrapolation accuracy is difficult to guarantee, based on the actual wind measurement data of offshore wind tower, the evaluation parameters and model of offshore wind resources are comprehensively analyzed and studied, and the offshore wind profile model based on neutral equivalent wind speed is proposed, and the following conclusions are drawn:

1) The characteristics of offshore wind resources are obviously different from those of onshore wind resources, mainly manifested in high average wind speed, low wind shear, and continuous change of ocean surface dynamic roughness. Therefore, the research method of temporal and spatial distribution of onshore wind resources is not applicable to offshore, and it is not suitable to use onshore wind shear model to fit offshore wind profiles.

2) In the offshore wind measurement stage, in addition to measuring the wind speed and direction at different heights, the temperature at least two altitude levels should also be measured to calculate the atmospheric stability parameters and improve the accuracy of wind resource assessment.

3) The atmospheric state is changing all the time, and the proportion of neutral state is small. The proportion of temperature inversion will also affect the distribution of atmospheric stability, and then

affect the distribution of offshore wind resources.

4) An offshore wind profile model based on neutral equivalent wind speed is proposed. The root mean square error and mean absolute error of extrapolated hub height are 0.43m/s and 0.28m/s, respectively, which are lower than the traditional extrapolation method, and provide a reference for the practical application of wind resource assessment engineering.

Acknowledgement

This research was not funded by any grant.

Conflicts of Interest

The authors declare no conflicts of interest.

References

[1] Carvalho, D., Rocha, A., Gómez-Gesteira, M., & Santos, C. S. (2014). Sensitivity of the wrf model wind simulation and wind energy production estimates to planetary boundary layer parameterizations for onshore and offshore areas in the iberian peninsula. *Applied Energy*, *135*, 234–246. https://doi.org/https://doi.org/10.1016/j.apenergy.2014;08.082

[2] Charnock, H. (1955). Wind stress on a water surface. *Quarterly Journal of the Royal Meteorological Society*, *81*(350), 639–640. https://doi.org/https://doi.org/10.1002/qj.49708135027

[3] Chen, W.-L., Zhang, Z., Liu, J., & Gao, D. (2025). Experimental study on dynamic characteristics of a jacket-type offshore wind turbine under coupling action of wind and wave. *Applied Energy*, *378*, 124876. https://doi.org/https://doi.org/10.1016/j.apenergy.2024.124876

[4] Fang, L., He, B., & Yu, S. (2025). A modular multi-step forecasting method for offshore wind power clusters. *Applied Energy*, *380*, 125060. https://doi.org/https://doi.org/10.1016/j.apenergy.2024.125060

[5] Jimenez, A., Crespo, A., Migoya, E., & García, J. (2008). Large-eddy simulation of spectral coherence in a wind turbine wake. *Environmental Research Letters*, *3*(1), 015004. https://doi.org/https://doi.org/10.1088/1748-9326/3/1/015004

[6] Jin, J., Li, Y., Ye, L., Xu, X., & Lu, J. (2023). Integration of atmospheric stability in wind resource assessment through multi-scale coupling method. *Applied Energy*, *348*, 121402. https://doi.org/https://doi.org/10.1016/j.apenergy.2023.121402

[7] Johnson, H., Højstrup, J., Vested, H., & Larsen, S. E. (1998). On the dependence of sea surface roughness on wind waves. *Journal of physical oceanography*, *28*(9), 1702–1716. https://doi.org/https://doi.org/10.1175/1520-0485(1998)028⟨1702:OTDOSS⟩2.0.CO;2

[8] Large, W., & Pond, S. (1981). Open ocean momentum flux measurements in moderate to strong winds. *Journal of physical oceanography*, *11*(3), 324–336. https://doi.org/https://doi.org/10.1175/1520-0485(1981)011⟨0324:OOMFMI⟩2.0.CO;2

[9] Lee, N., Woo, J., & Kim, S. (2025). A deep reinforcement learning ensemble for maintenance scheduling in offshore wind farms. *Applied Energy*, *377*, 124431. https://doi.org/https://doi.org/10.1016/j.apenergy.2024.124431

[10] Melalkia, L., Berrezzek, F., Saim, A., Nebili, R., et al. (2025). A hybrid error correction method based on eemd and convlstm for offshore wind power forecasting. *Ocean Engineering*, *325*, 120773. https://doi.org/https://doi.org/10.1016/j.oceaneng.2025.120773

[11] Peng, H., Zhong, B., Hu, G., & Liu, H. (2022). Optimization analysis of straight-bladed vertical axis wind turbines in turbulent environments by wind tunnel testing. *Energy Conversion and Management*, *257*, 115411. https://doi.org/https://doi.org/10.1016/j.enconman.2022.115411

[12] Radünz, W. C., Sakagami, Y., Haas, R., Petry, A. P., Passos, J. C., Miqueletti, M., & Dias, E. (2020). The variability of wind resources in complex terrain and its relationship with atmospheric stability. *Energy Conversion and Management*, *222*, 113249. https://doi.org/https://doi.org/10.1016/j.enconman.2020.113249

[13] Smith, S. D. (1988). Coefficients for sea surface wind stress, heat flux, and wind profiles as a function of wind speed and temperature. *Journal of Geophysical Research: Oceans*, *93*(C12), 15467–15472. https://doi.org/https://doi.org/10.1029/JC093iC12p15467

[14] Sørensen, P., Hansen, A. D., & Rosas, P. A. C. (2002). Wind models for simulation of power fluctuations from wind farms. *Journal of wind engineering and industrial aerodynamics*, *90*(12-15), 1381–1402. https://doi.org/https://doi.org/10.1016/S0167-6105(02)00260-X

[15] Wu, J. (1980). Wind-stress coefficients over sea surface near neutral conditions—a revisit. *Journal of Physical Oceanography*, *10*(5), 727–740. https://doi.org/https://doi.org/10.1175/1520-0485(1980)010⟨0727:WSCOSS⟩2.0.CO;2

[16] Wu, J. (1982). Wind-stress coefficients over sea surface from breeze to hurricane. *Journal of Geophysical Research: Oceans*, *87*(C12), 9704–9706. https://doi.org/https://doi.org/10.1029/JC087iC12p09704

[17] Yang, Z., & Dong, S. (2025). Modeling bivariate distribution of wind speed and wind shear for height-dependent offshore wind energy assessment. *Journal of Ocean University of China*, *24*(1), 40–62. https://doi.org/https://doi.org/10.1007/s11802-025-5830-2

[18] Yao, Q., Tang, J., Ke, Y., Li, L., Lu, X., Hu, Y., Fang, F., & Liu, J. (2024). Anti-tropical cyclone load reduction control of wind turbines based on deep neural network yaw algorithm. *Applied Energy*, *376*, 124329. https://doi.org/https://doi.org/10.1016/j.apenergy.2024.124329

[19] Yelland, M., & Taylor, P. K. (1996). Wind stress measurements from the open ocean. *Journal of Physical Oceanography*, *26*(4), 541–558. https://doi.org/https://doi.org/10.1175/1520-0485(1996)026⟨0541:WSMFTO⟩2.0.CO;2